Optical Materials 85 (2018) 127–132

Contents lists available at ScienceDirect

Optical Materials

journal homepage: www.elsevier.com/locate/optmat

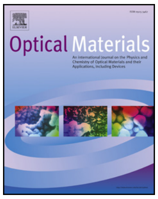

Spectroscopy of divalent samarium in alkaline-earth fluorides

E.A. Radzhabov[a,b,*]

[a] Vinogradov Institute of Geochemistry, Russian Academy of Sciences, Favorskii Street 1a, P.O.Box 4019, 664033 Irkutsk, Russia
[b] Irkutsk State University, Physics Department, Gagarin Boulevard 20, 664003 Irkutsk, Russia

ARTICLE INFO

Keywords:
CaF_2
SrF_2
BaF_2
Samarium
Absorption
Emission
Time-resolved
Spectroscopy

ABSTRACT

Optical spectra (absorption, luminescence, decay of emission, spectra with time resolution) of Sm^{2+} ions in alkaline-earth fluoride crystals (CaF_2, SrF_2, BaF_2) in the wavelength range 120–900 nm at 7–300 K were studied. By additive coloration of about 60% of the original Sm^{3+} is converted to Sm^{2+}.

One component of the decay of the Sm^{2+} emission was observed in BaF_2 crystals with a lifetime of 16 ms (a slow component) and in CaF_2 crystals with a lifetime of 1.3 μs (fast component) at low temperature. In SrF_2 crystals, two decay of luminescence components are found in the millisecond and nanosecond time range. The luminescence spectra of the slow and fast components in CaF_2, SrF_2, BaF_2 are similar, which confirms their attribution to forbidden 4f-4f and allowed 5d-4f transitions, respectively. The results obtained made it possible to clarify the position of the excited levels of Sm^{2+} 4f($^5D_0$) and 5d(e_g) relative to the bottom of the conduction band of alkaline-earth fluorides.

1. Introduction

Samarium ions are introduced into alkaline earth fluorides in forms 2 + or 3+. Both ions effectively luminesce. The emission of Sm^{2+} is observed only at low temperatures, Sm^{3+} also luminescent at room temperature. The spectroscopy of divalent samarium was studied by several scientific groups in the 1960s [1,2] in connection with the development of laser technology. Decay of emission [3,4] and vibronic spectra were thoroughly studied. In recent studies, CaF_2-Sm^{2+} crystals were considered as effective red x-ray scintillator [5]. Formation of divalent Sm in CsBr-Sm^{3+} is expected to be use in radio-photoluminescent dosimetry [6].

The main topic of the present paper is to establish the processes of changing the valence of Sm^{3+} ions by additive coloration and to determine the positions of the excited $4f^6$ and $4f^5 5d^1$ -levels within bans gap of alkaline earth fluoride crystals.

2. Experimental

Crystals were grown in vacuum in a graphite crucible by the Stockbarger method [7]. The graphite crucible contained three cylindrical cavities with a diameter of 10 mm and a length of 80 mm, which made it possible simultaneously to grow three samples with sizes Ø10 × 50 mm with different amounts of SmF_3. A few percent of CdF_2 were added into raw materials for purification from oxygen impurity during growth.

Crystals BaF_2, SrF_2, CaF_2 with 0.01, 0.03, 0.1 mol.% of SmF_3 were grown. All samarium was in trivalent form. For the transformation of samarium ions into a divalent form, an additive coloration procedure was used.

Absorption spectra in the range 190–3000 nm were taken with spectrophotometer Perkin-Elmer Lambda-950, emission spectra were measured using grating monochromator MDR2 (LOMO). Emission, excitation spectra were measured with photomultiplier tube module Hamamatsu H6780-04 (185–850 nm). No emission spectrum correction needs to be performed as the sensitivity only weakly changed in the region of emission (400–800 nm).

3. Results

3.1. Mechanism of conversion (Sm^{3+} to Sm^{2+})

Additive colouring of the crystals was carried out in an autoclave made of stainless steel at temperatures of 700–850°C. Samples of the crystals and pieces of metallic calcium were placed in different containers or separated by metal foil in the same container. After evacuation to 10^{-2}-10^{-3} Torr, the temperature increased up to 400°C. The samples were annealed at this temperature while pressure does not decrease down to 10^{-2} torr again. After heating to coloration temperature, the autoclave with the samples was kept in the oven for

---

* Vinogradov Institute of Geochemistry, Russian Academy of Sciences, Favorskii street 1a, P.O.Box 4019, 664033 Irkutsk, Russia.
E-mail address: eradzh@igc.irk.ru.

https://doi.org/10.1016/j.optmat.2018.08.044
Received 26 December 2017; Received in revised form 8 April 2018; Accepted 17 August 2018

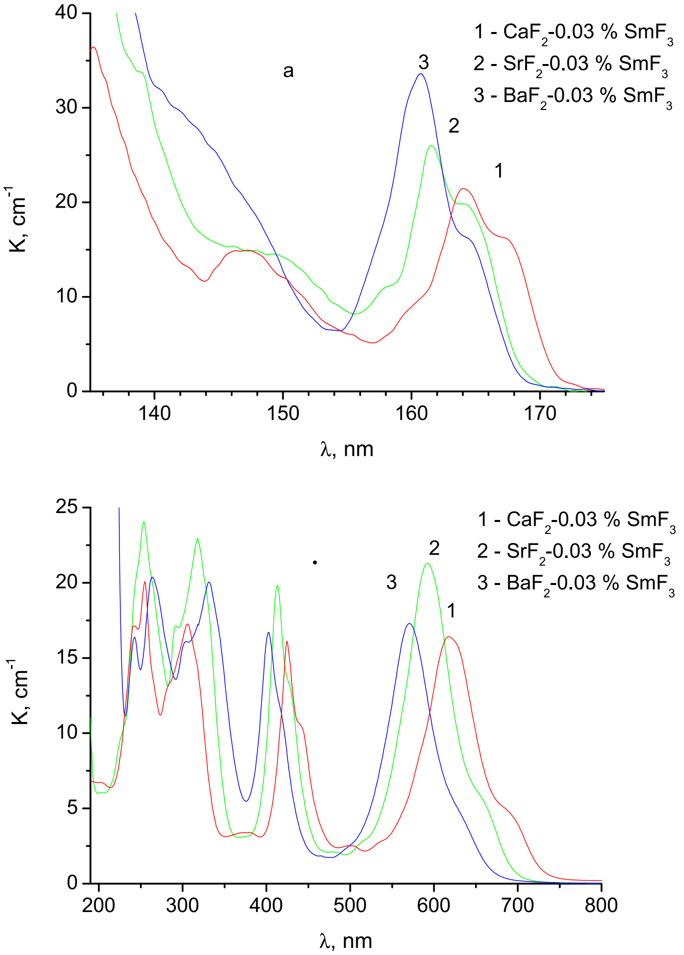

Fig. 1. Absorption spectra of initial (a) and additively coloured (b) MeF_2-0.03 mol. % SmF_3 crystals.

0.5–3 h, depending on the thickness of the samples, samarium contamination and temperature. After coloration samples were polished.

As a result of additive colouring, initially colourless crystals of alkaline-earth fluorides acquired a colour, the saturation of which increased with increasing initial concentration of trivalent samarium. In the absorption spectra (Fig. 1), characteristic bands of divalent samarium [1] appeared.

A linear dependence of the 4f-5d absorption bands of Sm^{3+} before coloration and Sm^{2+} bands after additive coloration was observed. The absorption coefficients of the allowed 4f-5d transitions of the initial Sm^{3+} and the formed Sm^{2+} are close in magnitude (see Fig. 1), which indicates that a significant fraction of initial trivalent samarium ions has become divalent.

The linear increase in the absorption coefficient of the Sm^{2+} long-wave band as a function of the concentration of the introduced SmF_3 is shown in Fig. 2. A similar dependence is also observed for other absorption bands of Sm^{2+} in the 200–500 nm region. It is known that in the crystal CaF_2-0.01 mol. % Sm^{2+} the absorption coefficient in the Sm^{2+} long wavelength band near 600 nm is equal to 9.3 cm^{-1} [8]. From this, one can draw the lines of the complete (100%) transformation $Sm^{3+} \rightarrow Sm^{2+}$ on Fig. 2. One can see that about 60% of the original trivalent samarium is converted into a divalent form by additive coloration of the alkaline-earth fluoride crystals (see Fig. 2).

The molar absorption coefficients of Sm^{2+} in SrF_2 and BaF_2 crystals are still unknown. Based on the results presented on Fig. 2 it can be assumed that the molar absorption coefficients of Sm^{2+} in three crystals of CaF_2, SrF_2 and BaF_2 are close.

Intensive absorption bands in the vacuum ultraviolet region are found in additively coloured SmF_3-doped CaF_2, SrF_2, and BaF_2 crystals at 161.0, 175.4, 206.0 nm, respectively. The bands belong to hydrogen H^- *a*-centres [9,10]. The formation of hydrogen centres is also confirmed by the appearance of the EPR signal of interstitial hydrogen atoms after X-ray irradiation of additively coloured crystals [10] and by infrared vibronic absorption bands near 794, 884, 957 cm^{-1} in BaF_2, SrF_2, CaF_2 respectively.

Additive coloration is due to the "dissolution" of metal atoms - the

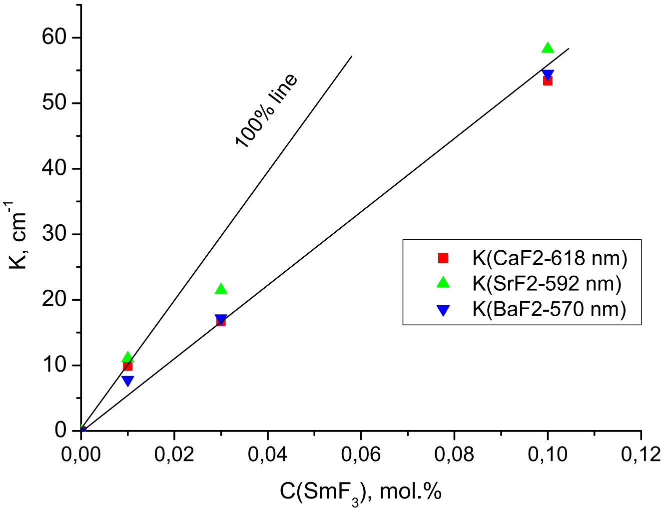

Fig. 2. The dependence of the magnitude of the long-wave Sm^{2+} band in coloured crystals on the concentration of SmF_3 in the original crystals.

addition of a metal ion from the vapour to the cation site on the crystal face and the motion of the formed anion vacancies and electrons deep into the crystal [11,12]. Thus, the additive coloration processes can be described by the following reactions:

$$(Sm^{3+}\text{-}F_i^-) + (V_a^- + e^-) \rightarrow Sm^{2+} \quad (1)$$

$$H_i^0 + V_a^- + e^- \rightarrow H_a^- \quad (2)$$

In equation (1), the interstitial fluorine ion, which is the charge compensator of trivalent samarium, falls into the anion vacancy while the electron converts the samarium ion to a divalent state.

In equation (2), the interstitial hydrogen atom, embedded in the crystal from the surrounding atmosphere, falls into an anionic vacancy and trapping the electron becomes a highly stable hydrogen ion H^-a.

Hydrogen diffused into crystal much more slowly than the anion vacancies [10], therefore the hydrogen absorption could be reduced by polishing the samples. It seems, the penetration of hydrogen from the atmosphere occurs with all methods of additive colouring. The source of hydrogen in the ambient vacuum can be water vapour [13] or organic impurities [10]. The energy of the interband transitions (band gaps) in the crystals of CaF_2, SrF_2, BaF_2 from the reflection spectra was determined to be 12.1, 11.25, 11.0 eV, respectively [14]. The position of the hydrogen band in the far ultraviolet region hampered the discovery of this process in the past (a few exceptions are [10,15]).

3.2. Absorption spectra

The absorption spectra of ions Sm^{2+} in the crystals CaF_2, SrF_2, BaF_2 have been studied in a number of papers [1,2]. The spectra contain a several broad absorption bands in the spectral range from 600 nm to 200 nm (see Fig. 1).

We observed prominent peaks at 338, 292, 248 cm^{-1} from zero phonon lines in $4f(^7F_0) \rightarrow 5d$ absorption spectra at 7.5 K of the CaF_2, SrF_2, BaF_2 respectively (Fig. 3). In the BaF_2 crystal, absorption bands are broad, but a comparison with the CaF_2, SrF_2 crystals makes it possible to determine their position (see Fig. 3). The smoothed absorption 4f-5d bands in BaF_2 are evidently caused by the location of the 5d level within the conduction band. The peaks 338, 292, 248 cm^{-1} in MeF_2-Sm^{2+} is closed to raman peaks 330, 290, 249 cm^{-1} of undoped alkaline-earth crystals at 77 K [16]. The weaker vibronic peak of 25 cm^{-1} longer wavelength was observed also (see Fig. 3). It has been found before that Raman active phonons are responsible for one of the major peaks observed in the emission vibronic spectra of Sm^{2+} activated crystals of the fluorite structure [17,18]. We observe similar transitions in absorption spectra also.

3.3. Emission

The emission spectrum of Sm^{2+} ions in alkaline-earth fluoride crystals consists of a diffuse wing at 650–800 nm and a narrow line of about 700 nm (Fig. 4). Apparently broadband luminescence in crystals CaF_2 and SrF_2 at room temperature is due to transitions of 5d-4f in ions Sm^{2+} (see Fig. 3). A narrow line near 700 nm in BaF_2, SrF_2 at 80 K is undoubtedly due to 4f-4f ($^5D_0$-$^7F_0$) transitions in ions Sm^{2+} (see also [1,2]).

The largest line of luminescence in crystals CaF_2 at 710 nm is wider than the similar lines at 697 nm in SrF_2, BaF_2 and 15 nm shifted relative to them. Such properties are not characteristic for the line of f-f transitions. Perhaps the line at 710 nm in CaF_2 does not belong to f-f transitions of Sm^{2+}. In the next section it will be shown that the observed luminescence in CaF_2 is due to 5d-4f transitions in Sm^{2+}.

At 7.5 K, the steady-state emission spectrum of Sm^{2+} ions in SrF_2 crystals contains intensive narrow line of f-f transitions at 696 nm. With increasing temperature, the intensity of the line decreases strongly in the temperature range 45–90 K. At the same time, a broadband emission spectrum appeared. On the curves of, The activation energy of the temperature growth of the broadband spectrum and quenching of the 696 nm line is estimated to be 400 cm^{-1}. Assuming that the broadband spectrum is due to 5d-4f transitions and the line is due to 4f-4f transitions, we can identify the obtained energy as the energy gap between level $4f(^5D_0)$ and higher $5d(e_g$ -level. The magnitude of the thermal gap 400 cm^{-1} is close to the value of 460 cm^{-1} determined in paper [2] and the value of 432 cm^{-1} determined in the paper [19].

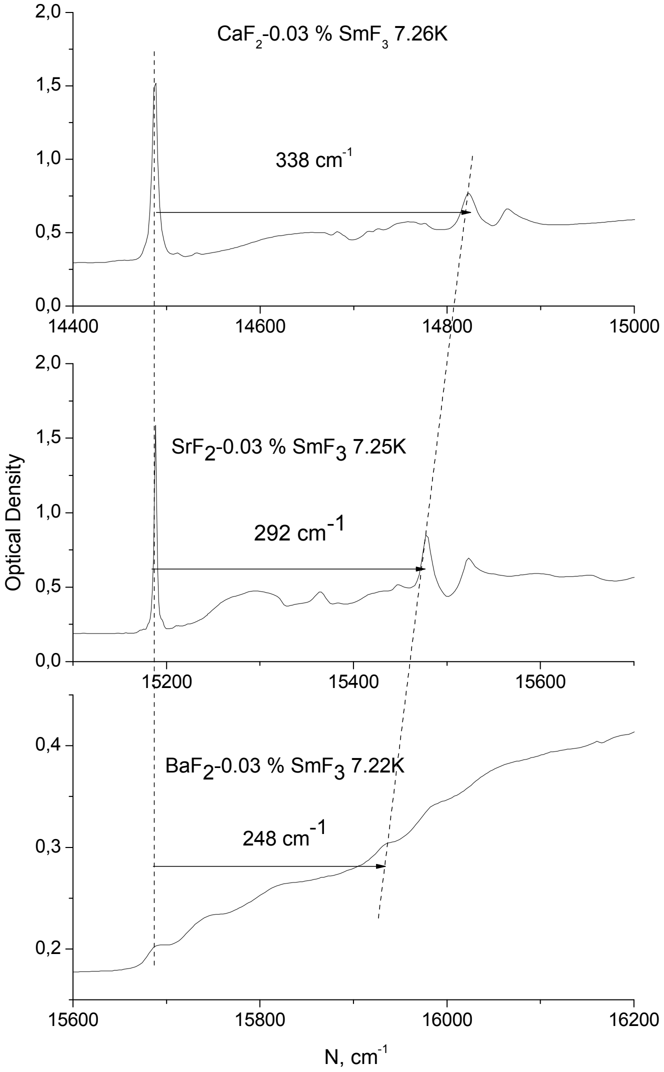

Fig. 3. Long-wavelength part of absorption spectra of MeF_2-Sm^{2+}. Positions of zero-phonon lines and Raman active mode are shown.

3.4. Time-resolved emission

The very different decay times of the broadband spectra, caused by allowed 5d-4f transitions, and line at 697 nm, which are due to forbidden 4f-4f transitions, were observed in SrF_2 [19–22]. To separate the allowed (fast) and forbidden (slow) emissions the time-resolved emission spectra were measured at 7–300 K. Obviously the fast and slow decay spectra in these crystals belong to 5d-4f and 4f-4f transition of Sm^{2+} ion respectively. The different emission spectra with fast and slow decay were observed in SrF_2-Sm^{2+} at 670–750 nm, while only slow decay spectra were observed in BaF_2-Sm^{2+} and only fast decay spectra were observed in CaF_2-Sm^{2+}.

The luminescence spectrum of the crystals BaF_2-Sm^{2+} (Fig. 5) does not change with time after the excitation pulse. In the temperature range 60–90 K, the integral intensity and the decay time (see the inset

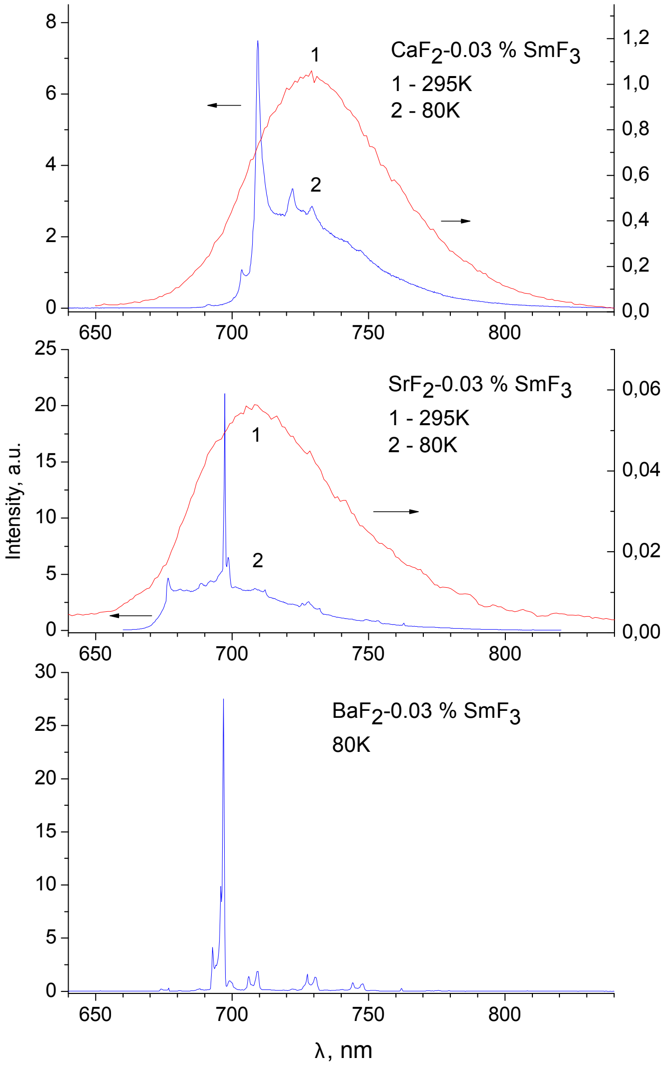

Fig. 4. Emission spectra of Sm^{2+} in alkaline-earth fluorides. Crystals BaF_2-Sm^{2+} did not have Sm luminescence at room temperature.

on Fig. 5) of the luminescence decrease in parallel. It follows that the 5d (e_g) level is substantially higher in energy than the 4f ($^5D_0$) level. The quenching is obviously connected with the thermal release of an electron from the $^5D_0$ level into the conduction band. According to the temperature dependence, we estimated the energy gap up to the bottom of the conduction band at 0.12 eV.

In the luminescence of SrF_2-Sm^{2+} crystals in an interval of 7–80 K, two decay components were observed: fast in the nanosecond range and slow in the millisecond range.

The lines at 675 and 697 nm observed in the fast and slow SrF_2-Sm^{2+} luminescence spectra, respectively (see Fig. 6). The luminescence spectrum of the fast component is more diffuse, which indicates a larger value of the electron-phonon interaction. The difference in the positions of the lines for the luminescence components is 467 cm^{-1}. The spectra of the vibronic wings for the luminescence components differ from each other, which indicates the prevalence of different phonon modes in the luminescence of both components. The luminescence spectra of the fast and slow SrF_2-Sm^{2+} component (see Fig. 6) are similar to the spectrum measured at the moment of excitation pulse and the integrated emission spectrum measured earlier [21].

At a temperature of 80 K, the line at 675 nm decreases significantly in the fast component spectrum and the structure of the spectrum becomes smoothed. In the spectrum of the slow component, a wing appears around 680 nm (see Fig. 6), apparently due to hot luminescence.

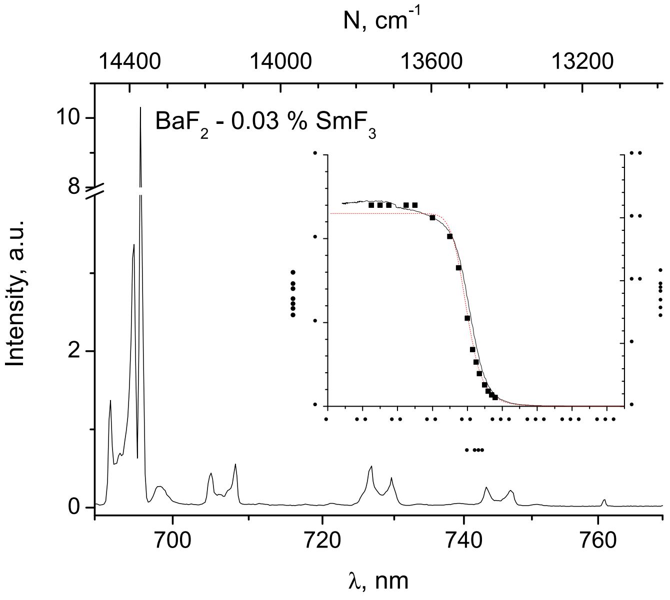

Fig. 5. The emission spectrum of BaF_2Sm^{2+} at 8.5 K. The inset shows the temperature dependence of the luminescence intensity (solid line) and the decay time (dots). The broken line shows the calculated curve for E = 0.12 eV and the frequency factor $4*10^7$ sec^{-1}.

The emission of Sm^{2+} in CaF_2 is characterized by a single exponent in the entire temperature range 7–300 K. At 7 K, the decay time is 1.3 microseconds. When heated, the intensity and decay time simultaneously decrease in the temperature range 160–300 K with an activation energy of 0.23 eV. The luminescence spectra measured at different times are close in shape (Fig. 7). It can be concluded that the luminescence of Sm^{2+} in CaF_2 is due to allowed 5d-4f transitions.

4. Discussion

The position of the levels of the lanthanides in the band scheme is determined in the Dorenbos model with an accuracy of 0.1–0.2 eV for many substances [23,24]. The position of the Sm^{2+} levels relative to the bottom of the conduction band in alkaline-earth fluorides was estimated in Ref. [23]. Nevertheless, experimental determination of the positions of the levels is important. Based on our experimental data, it is possible to clarify the position of the excited 5d and 4f levels of Sm^{2+} relative to the bottom of the conduction band of alkaline-earth fluorides.

The position of the excited levels of Sm^{2+} according to the Dorenbos model is shown in Fig. 8.

The Sm^{2+} ion has an electronic configuration of $4f^6$ in the ground state, and the ground multiplet can be designated ^7F_j(J = 0, …,6). The ground level is $^7F_0$ and first excited level is $^7F_1$. The distance between these two levels is determined to be 263 cm^{-1} in CaF_2 and SrF_2 as well as 278 cm^{-1} in BaF_2 [1,2]. Most intensive emission lines were observed for $^5D_0$ - $^7F_1$ and 5d(e_g) - $^7F_1$ transitions [1,2].

In the emission spectra of CaF_2 at 80 K from the short-wave side of the most intense 710 nm line, two lines of weak intensity were also observed at 703.5 and 691.5 nm (see Fig. 4). Upon cooling to 7 K, the lines at 703.5 and 691.5 nm disappeared. It can be assumed that they belong to transitions from higher levels, and the line at 710 nm is the line 5d(e_g)-4f($^7F_0$).

In CaF_2 crystals, the lowest excited level according to Dorenbos model is the $^5D_0$ level and the next 5d (e_g) level is 0.15 eV higher in energy.

The time-resolved emission spectra of Sm^{2+} in CaF_2 (see Fig. 7) correspond to the allowed 5d-4f transitions. The emission of ($^5D_0$-$^7F_1$) in CaF_2 crystals were not observed. The positions of 4f levels depend

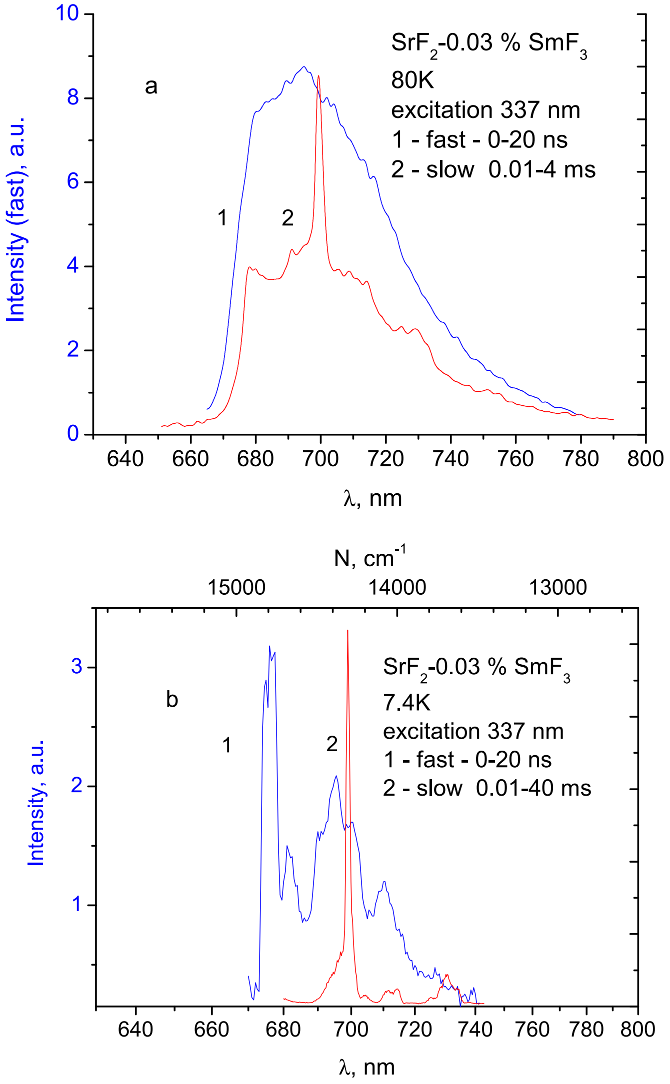

Fig. 6. The emission spectra with time resolution of SrF_2Sm^{2+} at 80 K (a) and 7.4 K (b). Intervals of the integration time for each spectrum with respect to the excitation pulse are shown in the figure.

weakly on the crystal environment. The lines in BaF_2, SrF_2 crystals were observed at 696.8 and 697.2 respectively (see Fig. 4). It can be estimated that the $^5D_0$-$^7F_1$ line in CaF_2 will be observed at about 697 nm, while the 5d-4f transition line is observed at 710.0 nm. Consequently, the level 5d(e_g) should be below the level 4f($^5D_0$) by 250 cm^{-1}, which is close to the value of 244 cm^{-1}, estimated using the Sm^{2+} level scheme from work [2]. The experimental position of 5d(e_g) of Sm^{2+} in CaF_2 is lower than the position estimated by the Dorenbos model by 1460 cm^{-1}.

In crystals of SrF_2-Sm^{2+}, at low temperatures, emission is observed from both the 5d(e_g) level and the 4f($^5D_0$) level. According to Dorenbos estimates, the lowest level of the excited level is the level $^5D_0$ and the next 5d(e_g) level is located at 0.25 eV (2016 cm^{-1}) higher in energy.

The maxima of the emission spectra of SrF_2-Sm^{2+} at 7.4 K of both decay components are shifted by 467 cm^{-1} from each other. It can be concluded that 5d(e_g) level is higher in the energy by 467 cm^{-1} than the $^5D_0$ level of Sm^{2+}. The energy gap between the two excited states is large enough so that there is no thermal equilibrium between the levels up to 80 K. Consequently, in accordance with the experimental results, it is necessary to reduce the energy gap between Sm^{2+} levels $^5D_0$ and 5d(e_g) in SrF_2 in the diagram of Fig. 8 to 467 cm^{-1}.

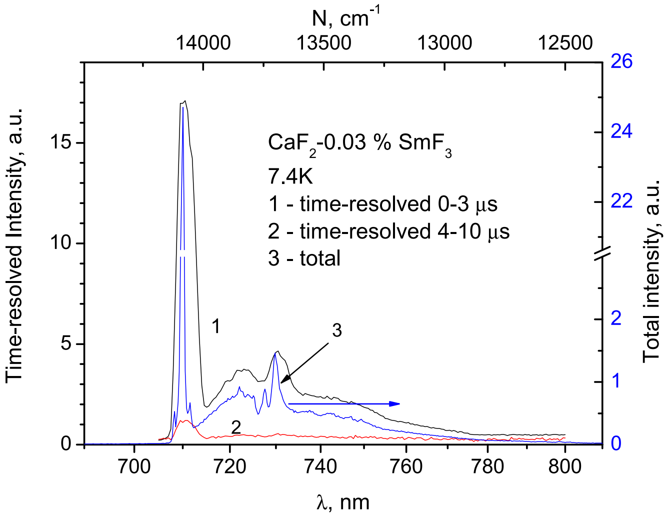

Fig. 7. Integral spectrum and luminescence spectra with a time resolution of CaF_2-Sm^{2+} at 7.4 K. The integration intervals for spectra with time resolution are indicated. One should pay attention to the discontinuity of the axis for the integral spectrum. Time-resolved spectra were measured with a larger spectral width of the monochromator slits than the width for the integral spectrum.

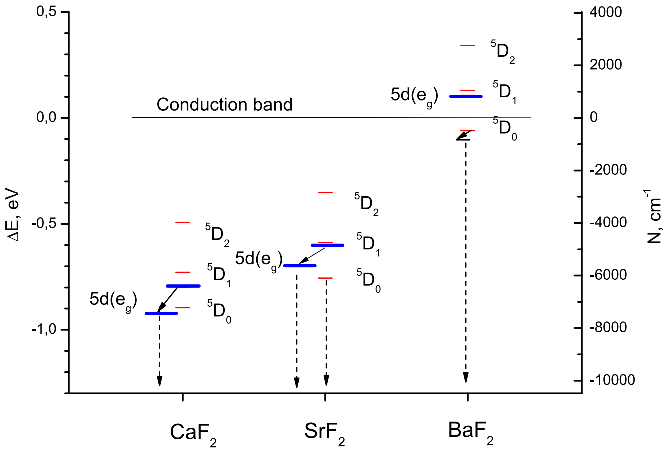

Fig. 8. Positions of 4f (^5D_i) and 5d(e_g) excited states of Sm^{2+} ions in alkaline earth fluorides taken from Dorenbos paper [25,26]. Vertical arrows show the observed radiative transitions to the ground level of $^7F_0$ of Sm^{2+} ions. The ground levels of the Sm^{2+} ion are at a distance of 2.71, 2.57, 1.88 eV below the bottom of the conduction band in CaF_2, SrF_2, BaF_2, respectively, and are not shown in the figure. The inclined arrows show the change in the position of the 5d(e_g) levels of CaF_2, SrF_2 and $4f^6$($^5D_0$) level of BaF_2 on the basis of our experimental results.

Due to the smaller splitting of the 5d states of the Sm^{2+} ion by the crystal field, the lowest level of 5d(e_g) rises higher in energy, which leads to an increase in the distance between 4f($^5D_0$) and 5d (e_g) in the series from CaF_2 to BaF_2. In BaF_2 crystals, the 5d(e_g) level shifts to the conduction band, which is reflected in the strong broadening of the absorption spectrum of BaF_2-Sm^{2+} (see Fig. 3). As a result of this, no emission of 5d(e_g)-4f($^7F_0$) was observed. The distance from the excited level $^5D_0$ to the bottom of the conduction band in the Dorenbos diagram is about 500 cm^{-1} (see Fig. 8).

The experimental temperature quenching of BaF_2-Sm^{2+} is described by a curve with an energy of 0.12 eV (968 cm^{-1}). Since the thermal quenching energy cannot be greater than the gap from $^5D_0$ to the bottom of the conduction band, the position of the $^7F_0$ ground level of Sm^{2+} in BaF_2 in the Dorenbos diagram should be lowered to a value of 880 cm^{-1} from bottom of conduction band.

5. Conclusion

Experimental results lead me to the following conclusion:

- A significant fraction of Sm^{3+} in alkaline-earth fluoride crystals is converted to a divalent state Sm^{2+} by additive coloration.
- Time-resolved emission measurements confirm that in CaF_2-Sm^{2+} only 5d-4f emission observed, in SrF_2 both 5d-4f and 4f-4f and in BaF_2 only 4f-4f emission observed.
- The position of the 5d(e_g) and 4f($^5D_0$) levels of Sm^{2+} of Dorenbos diagram should be slightly adjusted to match the experimental results.

Acknowledgments

The author gratefully acknowledge V.A. Kozlovskii for preparation the crystals investigated in this work and R. Schendrik for the measurement of IR spectra. The work was partially supported by RFBR grant 15-02-06666a and by the project of Russian Academy of Sciences 0350-2016-0024.

In this work author used the equipment of the Isotopic and Geochemistry Research Center for Collective Use, Institute of Geochemistry, Russian Academy of Sciences.

References

[1] D. Wood, W. Kaiser, Absorption and fluorescence of Sm^{2+} in CaF_2, SrF_2, and BaF_2, Phys. Rev. 126 (6) (1962) 2079–2088.
[2] P. Feofilov, A. Kaplyansky, Spectra of divalent rare-earth ions in alkaline-earth fluorides. 1. samarium, Optic Spectrosc. 12 (4) (1962) 493–500 in russian.
[3] F.K. Fong, H.V. Lauer, C.R. Chilver, M.M. Miller, Radiationless relaxation of rare-earth ions in solids: phenomenological effects of f f and f d transitions and the origin of multiphonon relaxation in first-order perturbation theory, J. Chem. Phys. 63 (1) (1975) 366–375.
[4] A.M. Alam, B. Di Bartolo, Thermal dependence of fluorescence and lifetimes of Sm^{2+} in several host lattices, J. Chem. Phys. 47 (10) (1967) 3790–3801.
[5] L.C. Dixie, A. Edgar, C.M. Bartle, Samarium doped calcium fluoride: a red scintillator and x-ray phosphor, Nucl. Instrum. Methods Phys. Res. Sect. A Accel. Spectrom. Detect. Assoc. Equip. 753 (2014) 131–137.
[6] G. Okada, Y. Fujimoto, H. Tanaka, S. Kasap, T. Yanagida, Sm-doped CsBr crystal as a new radio-photoluminescence (RPL) material, J. Rare Earths 34 (8) (2016) 769–773.
[7] E. Radzhabov, V. Nagirnyi, M. Kirm, E. Prosekina, 5d-4f emission of Nd^{3+}, Sm^{3+}, Ho^{3+}, Er^{3+}, Tm^{3+} ions in alkaline earth fluorides, Nucl. Sci. IEEE Trans. Nucl. Sci. 59 (2012) 2074–2078.
[8] V.A. Arkhangelskaya, M.N. Kiseleva, V. Schreiber, Molar absorption coefficients and oscillator strengths of some transitions to mixed (f-d) configurations of RE^{2+} ions in fluorite-type crystals, Optic Spectrosc. 23 (1967) 509–511 in russian.
[9] J. Beaumont, J. Gee, W. Hayes, Absorption in the vacuum ultraviolet of alkaline earth fluorides containing hydrogen, J. Phys. C Solid State Phys. 3 (8) (1970) L152.
[10] E.A. Radzhabov, A.V. Egranov, R.Y. Shendrik, Formation of H_a^- hydrogen centers upon additive coloration of alkaline-earth fluoride crystals, Optic Spectrosc. 122 (6) (2017) 901–905.
[11] N.F. Mott, R.W. Gurney, Electronic Processes in Ionic Crystals, second ed., University Press, Oxford, 1948.
[12] R. Pohl, Electron conductivity and photochemical processes in alkali-halide crystals, Proc. Phys. Soc. 49 (4S) (1937) 3.
[13] P. Lang, W. Knott, U. Werling, K. Renk, J. Campbell, G. Jones, Temperature dependence of the saturation of the h- local-mode absorption in caf 2 by use of a tunable carbon dioxide laser, Phys. Rev. B 44 (13) (1991) 6780.
[14] G.W. Rubloff, Far-ultraviolet reflectance spectra and the electronic structure of ionic crystals, Phys. Rev. B 5 (2) (1972) 662.
[15] W. Vehse, O. Facey, W. Sibley, Additive coloration of MgF_2, Physica Status Solidi (A) 1 (4) (1970) 679–683.
[16] R. Srivastava, H.V. Lauer, L.L. Chase, W.E. Bron, Raman frequencies of fluorite crystals, Phys. Lett. 36 (4) (1971) 333–334.
[17] D. Kuhner, M. Wagner, Lattice dynamics from vibronic spectra: examination of a generalized shell model for SrF_2 and BaF_2, Z. Phys. A: Hadrons Nucl. 256 (1) (1972) 22–42.
[18] E. Cohen, H.J. Guggenheim, Vibronic transitions of Sm^{2+} and Eu^{2+} in SrF_2 and their zeeman effect, Phys. Rev. 175 (2) (1968) 354–361.
[19] S.A. Payne, L.L. Chase, W.F. Krupke, L.A. Boatner, Excited state absorption of Sm^{2+} in SrF_2 and $SrCl_2$, J. Chem. Phys. 88 (11) (1988) 6751–6756.
[20] V. Bonch-Bruevich, I. Ignatiev, V. Ovsyankin, Spectrum and symmetry of vibrations forming the 4f5d-4f vibronic wing of the luminescence of MeF_2-RE^{2+} crystals. I.CaF_2-Sm^{2+}, Optic Spectrosc. 44 (3) (1978) 510–516 in russian.
[21] V. Bonch-Bruevich, I. Ignatiev, V. Ovsyankin, Spectrum and symmetry of vibrations forming the 4f5d-4f vibronic wing of the luminescence of MeF_2-RE^{2+} crystals. II.SrF_2-Sm^{2+}, Optic Spectrosc. 44 (4) (1978) 734–739 in russian.
[22] L. Chase, S.A. Payne, G.D. Wilke, Optical properties and nonradiative decay of Sm^{2+} in CaF_2-YF_3 and CaF_2-LaF_3 mixed crystals, J. Phys. C Solid State Phys. 20 (7) (1987) 953–965.
[23] P. Dorenbos, f d transition energies of divalent lanthanides in inorganic compounds, J. Phys. Condens. Matter 15 (3) (2003) 575.
[24] P. Dorenbos, Anomalous luminescence of Eu^{2+} and Yb^{2+} in inorganic compounds, J. Phys. Condens. Matter 15 (17) (2003) 2645.
[25] P. Dorenbos, Modeling the chemical shift of lanthanide 4 f electron binding energies, Phys. Rev. B 85 (16) (2012) 165107.
[26] P. Dorenbos, Charge transfer bands in optical materials and related defect level location, Opt. Mater 69 (2017) 8–22.